sciendo

Management Systems in Production Engineering

2024, Volume 32, Issue 4, pp. 555-562

Date of submission of the article to the Editor: 12/2023
Date of acceptance of the article by the Editor: 10/2024

DOI 10.2478/mspe-2024-0053

3D PRINTED STENT FROM GRAPHENE-POLYETHYLENE GLYCOL DIACRYLATE USING DIGITAL LIGHT PROCESSING TECHNIQUE

Farid Wajdi
Universitas Serang Raya

Alva Edy Tontowi
Universitas Gadjah Mada

Abstract:
This paper presents the development of the photocurable resin material based on the graphene reinforced polyethylene glycol diacrylate (gPEGDA) for vascular stent fabrication using a commercial 3D printer. 3D printing with digital light processing (DLP) technique is an attractive alternative for low-cost fast fabrication with high accuracy. Four photocurable resin compositions were prepared by mixing PEGDA and varied composition of graphene and the photoinitiator according to the design of experiment of 22 full factorial design. The diphenyl (2,4,6-trimethylbenzoyl) phosphine oxide (TPO) photoinitiator was adopted to meet the required 405 nm UV-light source wavelength of the 3D printer for stent fabrication. Material characterization of the UV-absorbance and viscosity tests were conducted and optimized to obtain resin printability. Mechanical characteristics tests were conducted to obtain the best resin composition for stent application. For this purpose, the tensile tests were conducted according to the ASTM D638 standard using the type-V specimen size. The test specimens were 3D printed with varied UV exposure time 20 and 30 seconds. Finally, the stents were successfully fabricated using a commercial 3D printer DLP with the bottom parameter time setting of 60 seconds, and the UV exposure time of 30 seconds. The resin material was applicable for 3D printing of the stent. The result has shown that 3D printer with DLP technique is suitable for stent fabrication with excellent surface quality. Moreover, the innovative bioresorbable stent materials and fabrication approach could open up new possibilities in the development of medical devices, particularly in the treatment of vascular diseases.

Key words: 3D printing, stents, pegda, graphene, photopolymer

INTRODUCTION

Stent placement is as an effective and minimally invasive vascular intervention to widen clogged blood vessels. Stent placement requires an experienced interventionist and a very flexible stent to maneuver within the blood vessels. Bioresorbable stents (BRS) are the latest stent technology in intervention for blocked vessels replacing permanent stents. The materials they are made off are designed to disintegrate within 3-6 months and to avoid irritating blood vessels. BRS offers significant advantages such as complete bio-resorption and mechanical flexibility. Poly-l-lactic acid (PLLA) is a common BRS material used for this vascular intervention. PLLA has excellent physical-chemical properties and is easy to deform [1, 2]. Furthermore, BRS can also be made from polyglycolic acid, polycaprolactone, polycarbonate, and a combination of them [3]. Oliviera et al. [4] emphasized the need for continued enhancements in this domain. These enhancements include minimizing thrombogenicity, lowering the strut thickness and reabsorption time, and enhancing the mechanical characteristics of the strut through the utilization of diverse polymers.

The current the production of commercial polymeric BRS involves melting and extruding the polymer to form thick-walled minitube. Subsequently, these tubes are heated beyond the glass transition temperature (Tg) and expanded into thin-walled minitube. Laser machining is then employed to cut these tubes [5]. Although the method delivers high accuracy of end products, it causes thermal and/or chemical defects at the machining sites. Even more, laser energy has a thermal and chemical effect on polymers [6]. Laser cutting of small and thin objects causes back wall damage which affects the surface quality and the risk of cracking [7], decrease in mechanical strength [8], and accelerates the degradation rate [9]. This method is very expensive due to required high laser energy and complex post-processing. 3D printing offers the opportunity to low-cost stent fabrication. Furthermore,

© 2024 Author(s). This is an open access article licensed under the Creative Commons BY 4.0 (https://creativecommons.org/licenses/by/4.0/)

3D printing allows to customize the stent size and make adjustments based on the patient's specific vessel characteristics. In current stenting practice, the stents are selected from the on-the-shelf available stent sizes. Since human anatomy varies, the customization of the stent size could potentially improve vessel patency. In this way, normal blood flow could be optimized [3].

The main techniques used for 3D printed stents are: fuse deposition manufacturing (FDM) and digital light processing (DLP). FDM and DLP, both exhibiting distinct advantages and drawbacks. When it comes to printing small devices, including vascular stents, the suitability of these technologies depends on several factors, including material selection, resolution, support structure, and printing speed. FDM typically utilizes various thermoplastic materials such as PLA, ABS, and others [10]. Although these materials are suitable for numerous applications, they may lack the necessary biocompatibility required for medical devices like vascular stents. While FDM can achieve respectable layer resolutions, the attainable level of detail might be constrained compared to alternative technologies like DLP [11]. This limitation could impact the precision required for complex structures, such as vascular stents. Moreover, FDM often requires support structures, posing challenges in their removal from complex designs like vascular stents, potentially affecting the overall quality and smoothness of the final printed object. FDM's relatively slower printing speed, constructing objects layer by layer [12], might be a noteworthy consideration for the time-sensitive production of small devices like vascular stents.

On the other hand, DLP can utilize a broader range of materials, including those with enhanced biocompatibility suitable for medical applications. This becomes particularly critical when printing devices like vascular stents, where the material must be safe for internal use in the human body. DLP excels in achieving very high resolutions up to 0.1 mm, enabling the fabrication of complex and detailed structure for small devices like vascular stents that demand precision [13]. Additionally, DLP often requires fewer or no support structures, leading to smoother and more detailed surfaces on the printed object, which is advantageous for complex structures like vascular stents. The generally faster printing speed of DLP, curing entire layers of resin at once, positions it as a more time-efficient option for the production of small devices, especially considering the time sensitivity in medical applications [13]. In conclusion, for the printing of small devices, particularly vascular stents, DLP emerges as a more suitable option due to its capability to deliver higher resolution, superior material choices for medical purposes, and faster printing speeds.

The aim of this study is to create composite stents using innovative material combinations involving graphene, PEGDA (Poly Ethylene Diacrylate) and TPO photoinitiator, employing 3D printing technology based on the DLP technique. The research includes an examination of the printability of the materials and their mechanical strengths. The physical characteristics of the material were examined through UV absorbance and viscosity tests. It was carried out to evaluate the suitability of the materials for the selected manufacturing method. Furthermore, the mechanical characteristics of the material were assessed by the tensile tests, which is crucial for confirming the materials' alignment with the requirements of BRS.

LITERATURE REVIEW

In recent years, the integration of 3D printing technology into the fabrication of stents has emerged as a transformative approach, holding the promise of enhanced customization, precision, and therapeutic outcomes. Van Lith et al. [3] developed a micro-Continuous Liquid Interface Production System (microCLIP) 3D printer with a 365 nm UV light source to make a self-expandable stent from methacrylated poly (1,12 Dodecamethylene Citrate) photopolymer resin. However, the use of Irgacure and Sudan I photoinitiators to confer photocurability upon the resin material renders it non-biocompatible due to its toxicity. Ware et al. [14] enhanced the result of the study to obtain a thinner stent strut and faster fabrication time up to 150 µm and 11.3 min, respectively.

FDM technique has been used in developing vascular stents by a number studies. Misra et al. [15] developed a self-expandable stent using an FDM 3D printer from polycaprolactone-graphene nanocomposite filament material of 2 mm diameter. They constructed the stent model for the first time based on direct segmentation of medical images. The study has resulted a customized 3D printed stent with a diameter of 4 mm. Jia et al. [16], using a commercial 3D printer FDM (F3CL, Panowin Instruments) to develop a self-expandable stent from self-memory polylactic acid (PLA) filament material. The 3D printed stent has original diameter, length, thickness, rib width, and rib length are 4.0 mm, 40.0 mm, 0.4 mm, 0.5 mm, and 1.0 mm, respectively. This study focused on the mechanism of self-expandable stents. However, the PLA material biocompatibility is not discussed in this study. Another attempt to the vascular stent development using 3D printing technology was conducted by Qiu et al. [17]. They have effectively created an innovative bioresorbable polymeric stent using Polycaprolactone (PCL) and modified sulphated chitosan (CS). A rotary 3D printing technique is employed for the production of these polymeric stents. The outcomes of physical and chemical characterization indicate that the surface microstructure of 3D-printed PCL stents can be impacted by CS modification, although there is no noteworthy difference in their mechanical performance.

The above-mentioned studies demonstrate various efforts in the development of 3D printed vascular stents, utilizing both FDM and DLP techniques. Some aim to innovate new stent materials that can offer clinical advantages, while others focus on optimizing 3D printing parameters to achieve optimal fabrication of vascular stents. Compared to FDM, the DLP technique shows a better accuracy and better surface quality [18]. However, the use of a DLP 3D printer for stent manufacturing requires a biocompatible photocurable resins and meets the material

strength required to open clogged vessels. One of the resin materials that potentially can be used for the manufacturing of stents is Polyethylene Glycol Diacrylate (PEGDA). PEGDA is an acrylate-based prepolymer that is widely used in the photopolymerization process with a short reaction time [19]. PEGDA is biocompatible, soluble in water and organic solvents, odorless, non-volatile and non-irritating [20]. PEGDA has been approved by the US food and drug administration (FDA) as a safe, biocompatible, non-immunogenic, and has been used in many applications in human [21]. To increase the mechanical strength of PEGDA, graphene was added. Graphene is an allotrope of carbon with a 2D hexagonal structure, consisting of a single layer of sp2 bonds of carbon atoms. Graphene is a biocompatible material with low toxicity but its use as a medical implant material must be in very low concentrations [22, 23]. As recommended by Liao et al. [24], a safe concentration of graphene in blood is not to exceed 25 µg/ml.

Subsequently, DLP technique requires photocurable material for its fabrication process, the proposed materials should be made as photopolymers by adding photoinitiator. Photopolymers undergo chemical changes when exposed to light with a wavelength that matches the light absorbance spectrum of the photoinitiator [25]. The common wavelength of the light source used by the 3D printer machine is UV 405 nm [26, 27]. Hence, the careful choice of a photoinitiator that aligns with the specifications of the 3D printer is crucial. Diphenyl (2,4,6-trimethylbenzoyl) phosphine oxide (TPO) is selected as the photoinitiator for this study. TPO possesses the ability to convert double bonds in photopolymerization reactions, thus minimizing the occurrence of shrinkage in the printed outcomes and conveying favorable mechanical properties [25, 28]. TPO has the capability to generate radicals over a broader spectrum, particularly under UV light, making it suitable for application in the DLP technique. Given that the DLP system utilizes light within the range of 365 nm up to the near-infrared spectrum, the TPO photoinitiator demonstrates potential compared to other counterparts. Furthermore, TPO is well-tolerated by various cells, and its applicability, particularly in clinical practice, holds promise, contingent on concentration [29]. According to Wang et al. [30], a concentration of 1.0 wt% TPO is considered biocompatible when appropriately diluted with an equivalent volume of culture medium.

Once the material's wavelength aligns with that of the 3D printer machine, it is essential to modify the material viscosity to correspond with the kinetics of photopolymerization within the printing region [31]. The viscosity of a liquid is affected by temperature and pressure. The increase in temperature affects the decrease in viscosity. The increase in pressure affects the increase in viscosity [32]. 3D DLP printers require a low-viscosity resin so that the resin moves quickly in the printing area. High viscosity resin or too viscous will be difficult to flow in the printing area, causing printing failure [27]. Viscosity refers to the thickness or resistance to flow of a liquid. When the resin used in printing is highly viscous, it becomes difficult for it to flow smoothly in the printing area. As a result, the printing process fails, as the resin cannot spread evenly or adhere properly to the desired surface. To ensure successful printing, it is important to use a resin with an appropriate viscosity that allows for smooth and consistent flow.

This study introduces novelty in the development of graphene-based nanocomposite polymer stent materials applicable through the 3DP DLP technique. The nanocomposite graphene-based photopolymer resin represents a novel material composition in polymer stent development, previously unexplored. The application of 3DP DLP is a manufacturing method that proves to be more economical and flexible compared to FDM or even laser cutting methods. We present the development of photocurable resins material based on PEGDA, reinforced by graphene, and TPO photoinitiator. These materials are regarded as biocompatible and suitable for use in bio implant applications.

RESEARCH METHODOLOGY

Materials

Polyethylene glycol diacrylate (PEGDA, Mn. 575) and diphenyl (2,4,6-trimethylbenzoyl) phosphine oxide (TPO) photoinitiator were purchased from Sigma-Aldrich. Graphene powder were provided by Product Design Lab UGM, which was synthetized from natural graphite powder (60 mesh particle size, > 95% carbon), using mechanical exfoliation method [33].

Preparation of Photopolymer Resins

Prior to the resin preparation, the UV absorbance of the TPO photoinitiator was measured using a Shimadzu 1700 UV-Vis spectrophotometer (Shimadzu, Japan). The TPO photoinitiator was dissolved in acetone with a concentration of 0.01%. The UV spectroscopic measurement was set in the range of 350-450 nm of wavelength. The photocurable resins were prepared by mixing graphene and PEGDA for 30 minutes using a magnetic stirrer WiseStir MSH 20D (Wise, Japan). The TPO photoinitiator was added into the suspension and sonicated for 30 minutes using a water-bath sonicator 40 Hz Branson 3800 (Branson, USA) to create a homogenous photocurable resin.

Table 1
Design experiment of the photopolymer resin preparation

Run	A	B	PEGDA (ml)	Graphene (g)	TPO (g)
1	-	-	10	0.01	0.05
2	+	-	10	0.03	0.05
3	-	+	10	0.01	0.1
4	+	+	10	0.03	0.1
5	-	-	10	0.01	0.05
6	+	-	10	0.03	0.05
7	-	+	10	0.01	0.1
8	+	+	10	0.03	0.1
9	-	-	10	0.01	0.05
10	+	-	10	0.03	0.05
11	-	+	10	0.01	0.1
12	+	+	10	0.03	0.1

A = graphene, B = TPO

The composition of graphene and TPO photoinitiator was varied for each of 10 ml PEGDA. The experiments were run according to the Full Factorial Design 2^2 in triplicate, as shown in Table 1.

Characterizations

The viscosity of the resins was measured by a Labo viscometer (Labo, China) at room temperature (25°C). The mechanical properties were examined by tensile test using a Hung Ta HT-2402 (Hung Ta, Taiwan) material testing machine with a load capacity of 5 KN, tensile rate of 10 mm/min, in a conditioned room of 23°C, 50 RH. The tensile test specimens were 3D printed horizontally using Anycubic Zero 3D DLP printer (Anycubic Shenzen Technology, China), as shown in Fig. 1. The tensile tests were conducted according to the ASTM D638 standard and type-V specimen size.

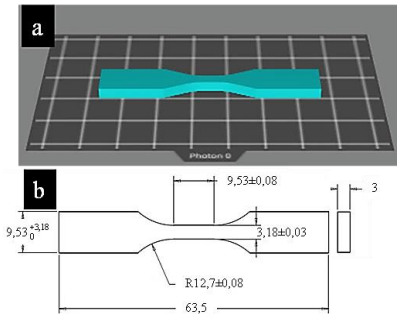


Fig. 1 Type-V ASTM 638 specimen for tensile test

Fractional Factorial Design (FFD) of 2^{3-1} was applied to run the experiment. The variables were graphene (%wt), photoinitiator (%wt), and the exposure time (second). The factors and levels in this experimental design are shown in Table 2.

The FTIR test was carried out to determine the structure of the chemical bond after curing. The FTIR spectra were obtained from a Shimadzu IRPrestige spectrophotometer (Shimadzu, Japan).

Table 2

The variables of the tensile test specimens

Run	A	B	C	Graphene (%wt)	TPO (%wt)	Exposure Time (s)
1	-	-	+	0.1	0.5	30
2	+	-	-	0.3	0.5	20
3	-	+	-	0.1	1	20
4	+	+	+	0.3	1	30
5	-	-	+	0.1	0.5	30
6	+	-	-	0.3	0.5	20
7	-	+	-	0.1	1	20
8	+	+	+	0.3	1	30
9	-	-	+	0.1	0.5	30
10	+	-	-	0.3	0.5	20
11	-	+	-	0.1	1	20
12	+	+	+	0.3	1	30

A = graphene, B = TPO, C = exposure time

Stent Fabrication

The 3D DLP printer, Anycubic Zero (Shenzen Anycubic Technology, China), was used to print the stent prototype from a 3D CAD stent model developed in our lab as shown in Fig. 2.

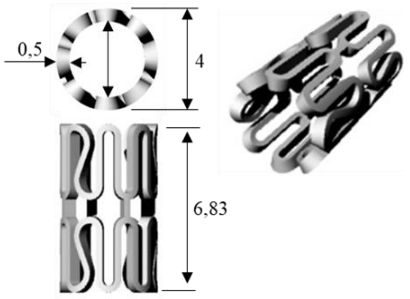


Fig. 2 3D CAD stent model

This machine is equipped with a 405 nm UV-LED light source. The dimension of the stent is 6.83 mm in length, 4 mm in diameter, and 0.5 mm in strut thickness.

RESULTS AND DISCUSSION

Photoinitiator UV-absorbance

The result of the UV absorbance measurement is shown in Fig. 3.

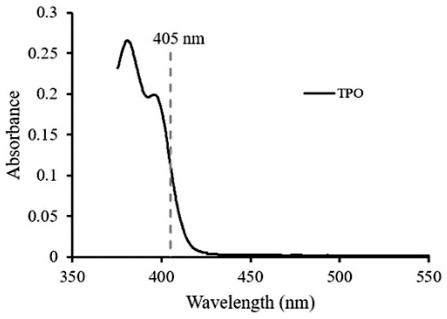


Fig. 3 UV absorbance of TPO photoinitiator

The TPO photoinitiator shows a significant UV absorbance at 405 nm, at the point 0.113. TPO plays a good role in double bond conversion and mechanical properties on resin materials [28]. High double bond conversion can prevent the shrinkage ratio of printed objects [25].

Photocurable Resins gPEGDA

Sonication of the PEGDA-graphene mixture resulted in a dark homogeneous suspension. Sonication treatment helps to prevent graphene agglomeration [34]. The graphene dispersion occurs by the cavitation energy and shear force of the ultrasonic waves generated by the sonicator [35]. After adding TPO to the suspension and followed by stirring, the obtained gPEGDA photopolymer resin was as shown in Fig. 4 for each composition.

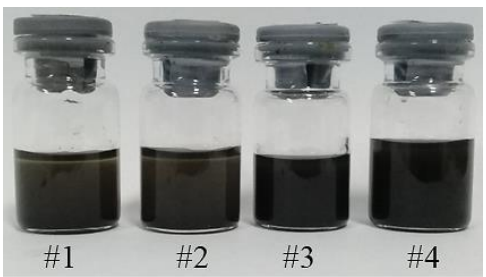


Fig. 4 Physical appearance of the developed gPEGDA resins

As shown in Fig. 4, there is almost no difference in the colour of the suspensions of each composition because there is only a slight difference (0.02 g) in the concentration of graphene in each resin composition. Graphene concentration was limited due to safety considerations when it enters human blood [24].

Viscosity

The viscosity tests on 4 resins compositions were conducted in 3 replications. The results of the tests are shown in Fig. 5. Resins composition # 1 and # 3 exhibited viscosities of 0.0510 Pa.s and 0.0512 Pa.s, respectively. Resins # 2 and # 4 exhibited viscosities of 0.0714 Pa.s and 0.0714 Pa.s, respectively. The resin viscosities were below the range of 0.25-1 Pa.s, meaning that the resins were fluid and would perform a good flow for printing [36].

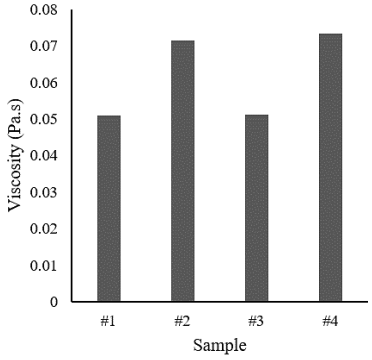


Fig. 5 Viscosity of the resins

The low viscosity of the resin allowed for a faster printing process by facilitating smooth flow through the printing area. Low-viscosity resins have good fluidity because they can flow to the printing area in time, while high-viscosity resins have poor fluidity which causes a decrease in print speed or print failure [27].

Mechanical Properties

The tensile test specimens were successfully printed according to the ASTM D638 Type-V standard. The specimens were printed horizontally using Anycubic Zero 3D DLP printer. The 3D printed test specimens are presented in Fig. 6.



Fig. 6 Tensile test specimens

Appropriate mechanical properties of 3D DLP printed stents are critical. We evaluated the mechanical strength of each resin by tensile test to obtain its modulus and tensile strength properties. The results are shown in Fig. 7.

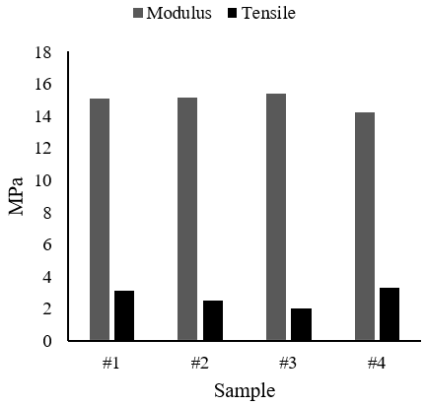


Fig. 7 The average of modulus and tensile strength

The Young's modulus response of the tensile test indicates material flexibility. The Young's modulus of samples #1 to #4 were 15.10 MPa (SD 0.207), 15.17 MPa (SD 0.567), 15.40 MPa (SD 0.551), 14, 25 MPa (0.364), respectively. ANOVA test showed that there is no interaction between variables graphene (A), TPO (B), and exposure time (C) for the modulus response. The exposure time variable (C) exhibited a significant effect on the modulus response ($p < 0.06$).

The maximum tensile response was obtained from sample #4, with an average of 3.32 MPa. The average tensile from the lowest to the highest was obtained from samples #3, #2, #1, #4, which were 2.03 MPa, 2.49 MPa, 3.11 MPa, and 3.32 MPa, respectively. This also shows that the average tensile strength of all samples has met the requirements for the mechanical strength of the stent of 40 kPa [37].

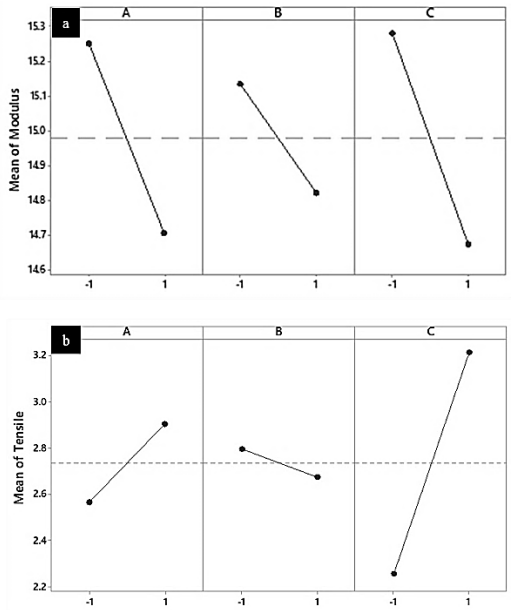


Fig. 8 The interaction of variables in (a) modulus and (b) tensile properties

The results of the ANOVA test showed no interaction between factors graphene (A), TPO (B), and exposure time (C) on the tensile response. Only the exposure time (C) had a significant effect on the tensile response ($p < 0.06$).

Meanwhile, the influence of graphene (A) and TPO (B) factors was not significant ($p > 0.06$). The relationship of each factor with the tensile response is shown by the main effect plot in Fig. 8.

Converting the nominal stress-strain values into the true stress-strain values defines the plastic behavior of the material. As a sample, Fig. 9 shows the nominal stress-strain curve of specimen #3 with 12.06 MPa of Young's modulus.

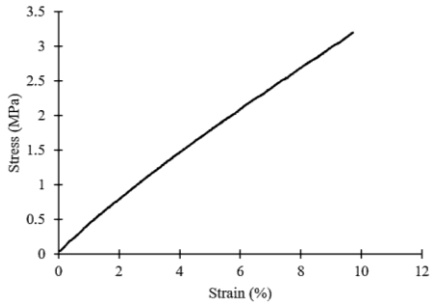


Fig. 9 Stress-strain curve of the tensile test specimen

Twelve points from the curve were converted to determine the plastic strain of the material. Table 3 shows that the plastic strain values for every point are around zero. It means that that the cured gPEGDA photopolymer exhibits elastic behavior.

Table 3
Conversion of the nominal stress-strain values to determine plastic strain

Points	Strain	Stress	True Strain	True Stress	Plastic Strain
1	0.08360	0.04407	0.08029	0.04776	0.07633
2	0.10060	0.05319	0.09586	0.05854	0.09100
3	1.05040	0.44530	0.71803	0.91304	0.64233
4	2.10440	0.82525	1.13282	2.56191	0.92039
5	3.72380	1.36934	1.55261	6.46848	1.01626
6	4.19740	1.52740	1.64816	7.93849	0.98991
7	5.40380	1.91266	1.85689	12.24832	0.84128
8	6.34420	2.19687	1.99391	16.13423	0.65608
9	7.01080	2.38760	2.08079	19.12660	0.49484
10	8.74420	2.89597	2.27667	28.21895	-0.06321
11	9.63100	3.16498	2.36377	33.64688	-0.42618
12	9.72400	3.19689	2.37248	34.28349	-0.47026

IR Spectra

FTIR (Fourier Transform Infrared Spectroscopy) is a technique used to identify the presence of certain chemical groups or functional groups in a sample.

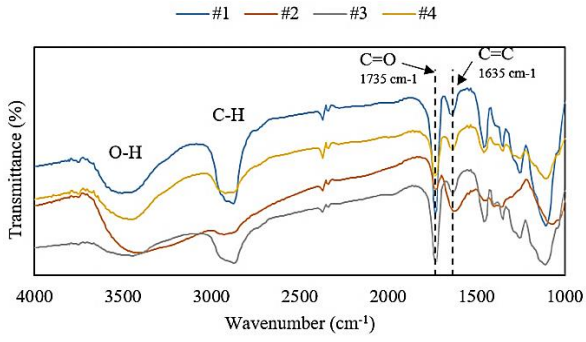


Fig. 10 IR spectra after curing

The FTIR spectra, depicted in Fig. 10, reveal specific vibrations at different wavenumbers that indicate the presence of certain chemical groups.

The vibration at 1735 cm^{-1} indicates the presence of the C = O ester group. The stretching observed at 3500-3400 cm^{-1} confirms the weakening of the O-H group, which is a result of the polyesterification process. Additionally, the conversion of C = C at 1635 cm^{-1}, C = O at 1735 cm^{-1}, and C-H at 2924-2870 cm^{-1} characterizes the bond between TPO and PEGDA.

Stent Fabrication

3D DLP printers operated well during the printing process and produced the stent prototypes as shown in Fig. 11.

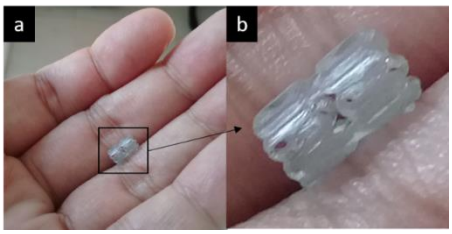


Fig. 11 3D Printed stent from resin #3 (a) in real size and (b) its magnificent

Resin #3 produced a stent prototype without defects. The exposure time parameters of 30 and 40 seconds were sufficient for printing the resins #1 and #3. However, it did not work properly for the resins #2 and #4. The defects occurring in both printed objects are attributed to a higher concentration of graphene in the resin (0.3%), hindering the absorption of UV light by the photoinitiator [34]. UV light irradiation is more absorbed by the darker-colored resin, while UV adsorption by the photoinitiator is also essential to initiate photopolymerization. Resin with a darker hue necessitates a longer exposure time for proper curing. Challenges of this nature can be addressed by employing a printer with higher UV light intensity [38]. The bottom exposure time parameter is intended to attach objects properly to the platform. At a bottom exposure time of 60 seconds, the object adheres to the platform well and is easier to remove from the platform. At the bottom exposure time parameter of 70 and 80 seconds, the printing object is more stable attached to the platform than at 60 seconds. In general, small and thin 3D objects used in this printing test can use all the parameters of the bottom exposure time. Based on considerations of time efficiency and security of attachment to the platform, the bottom exposure time parameter of 60 seconds is considered sufficient.

CONCLUSIONS

The outcomes of this investigation clearly demonstrate the successful fabrication of vascular stents using the developed photopolymer resin. The compositional makeup of the photopolymer aligns seamlessly with the mandated mechanical characteristics required for stent functionality. It is important that the findings from this study may be extrapolated to apply to various other polymer matrices, underlining the versatility and applicability of the

developed photopolymer. Particularly, the mechanical attributes of the resin exhibit a commendable combination of strength and flexibility, thereby meeting the stipulated requirements for radial stent strength. The material deposition showcases favorable flow characteristics, confirmed by a viscosity range of 0.051-0.071 Pa.s. It is imperative to acknowledge that at higher concentrations of graphene, an extended curing time is observed. This phenomenon can be attributed to the color density factor of the resin, which hinders the efficient absorption of UV light by the photoinitiator. In considering the broader implications of this research, several critical aspects emerge. The considerations for future studies should encompass a nuanced examination of stent design, degradation rate, post-processing methodologies to enhance surface quality, and a comprehensive analysis of printer specifications. These factors collectively contribute to the holistic understanding and advancement of 3D-printed vascular stents in both scientific and practical domains.

ACKNOWLEDGEMENT

We acknowledge the Post-Doctoral Program Universitas Gadjah Mada for supporting this research.

REFERENCES

[1] E.L. Boland, R. Shine, N. Kelly, C.A. Sweeney, and P.E. McHugh, "A Review of Material Degradation Modelling for the Analysis and Design of Bioabsorbable Stents," *Ann. Biomed. Eng.*, vol. 44, no. 2, pp. 341-356, 2016, doi: 10.1007/s10439-015-1413-5.

[2] D. Garlotta, "A Literature Review of Poly (Lactic Acid)," *J. Polym. Environ.*, vol. 9, no. 2, pp. 63-84, 2002, doi: 10.1023/A:1020200822435.

[3] R. van Lith *et al.*, "3D-Printing Strong High-Resolution Antioxidant Bioresorbable Vascular Stents," *Adv. Mater. Technol.*, vol. 1, no. 9, pp. 1-7, 2016, doi: 10.1002/admt.201600138.

[4] M.F. De Oliveira, L.C.E. Silva, and M.G. De Oliveira, "Bioprinting 3D printed bioresorbable nitric oxide-releasing vascular stents," *Bioprinting*, vol. 22, no. December 2020, p. e00137, 2021, doi: 10.1016/j.bprint.2021.e00137.

[5] R.D. Alexy and D.S. Levi, "Materials and Manufacturing Technologies Available for Production of a Pediatric Bioabsorbable Stent," vol. 2013, 2013.

[6] A.W. Martinez and E.L. Chaikof, "Microfabrication and Nanotechnology in Stent Design," *Wiley Interdiscip. Rev. Nanomedicine Nanobiotechnology*, vol. 76, no. October 2009, pp. 211–220, 2012, doi: 10.1007/s11103-011-9767-z.Plastid.

[7] N. Muhammad, "*Laser Micromachining of Coronary Stents for Medical Applications*," University of Manchester, 2012.

[8] N. Grabow, M. Schlun, K. Sternberg, N. Hakansson, S. Kramer, and K.-P. Schmitz, "Mechanical Properties of Laser Cut Poly(L-Lactide) Micro-Specimens: Implications for Stent Design, Manufacture, and Sterilization," *J. Biomech. Eng.*, vol. 127, no. 1, pp. 25-31, 2005, doi: 10.1115/1.1835349.

[9] A. J. Guerra and J. Ciurana, "Effect of fi bre laser process on in-vitro degradation rate of a polycaprolactone stent a novel degradation study method," *Polym. Degrad. Stab.*, vol. 142, pp. 42-49, 2017, doi: 10.1016/j.polymdegradstab.2017.05.028.

[10] M. Lalegani Dezaki, M. K. A. Mohd Ariffin, and S. Hatami, "An overview of fused deposition modelling (FDM): research, development and process optimisation," *Rapid Prototyp. J.*, vol. 27, no. 3, pp. 562-582, 2021, doi: https://doi.org/10.1108/RPJ-08-2019-0230.

[11] R.F. Quero, G. Domingos da Silveira, J.A. Fracassi da Silva, and D.P. de Jesus, "Understanding and improving FDM 3D printing to fabricate high-resolution and optically transparent microfluidic devices," *Lab Chip*, vol. 21, no. 19, pp. 3715-3729, 2021, doi: 10.1039/D1LC00518A.

[12] S. Deng, J. Wu, M. D. Dickey, Q. Zhao, and T. Xie, "Rapid Open-Air Digital Light 3D Printing of Thermoplastic Polymer," *Adv. Mater.*, vol. 31, no. 39, pp. 1-7, 2019, doi: 10.1002/adma.201903970.

[13] J. Fei *et al.*, "Progress in Photocurable 3D Printing of Photosensitive Polyurethane: A Review," *Macromol. Rapid Commun.*, vol. 44, no. 18, p. 2300211, Sep. 2023, doi: https://doi.org/10.1002/marc.202300211.

[14] H.O.T. Ware *et al.*, "High-speed on-demand 3D printed bioresorbable vascular scaffolds," *Mater. Today Chem.*, vol. 7, pp. 25-34, 2018, doi: 10.1016/j.mtchem.2017.10.002.

[15] S.K. Misra *et al.*, "3D-Printed Multidrug-Eluting Stent from Graphene-Nanoplatelet-Doped Biodegradable Polymer Composite," *Adv. Healthc. Mater.*, pp. 1-14, 2017, doi: 10.1002/adhm.201700008.

[16] H. Jia, S.Y. Gu, and K. Chang, "3D printed self-expandable vascular stents from biodegradable shape memory polymer," *Adv. Polym. Technol.*, vol. 37, no. 8, pp. 3222-3228, 2018, doi: 10.1002/adv.22091.

[17] T. Qiu, W. Jiang, P. Yan, L. Jiao, and X. Wang, "Development of 3D-Printed Sulfated Chitosan Modified Bioresorbable Stents for Coronary Artery Disease," *Front. Bioeng. Biotechnol.*, vol. 8, no. May, pp. 1-12, 2020, doi: 10.3389/fbioe.2020.00462.

[18] C. Schmidleithner and D.M. Kalaskar, "Stereolithography," in *3D Printing*, Intechopen, 2018, pp. 3-22.

[19] C. Mendes-Felipe, J. Oliveira, I. Etxebarria, J.L. Vilas-Vilela, and S. Lanceros-Mendez, "State-of-the-Art and Future Challenges of UV Curable Polymer-Based Smart Materials for Printing Technologies," *Adv. Mater. Technol.*, vol. 4, no. 3, pp. 1-16, 2019, doi: 10.1002/admt.201800618.

[20] S.C. Ligon *et al.*, "Polymers for 3D Printing and Customized Additive Manufacturing," *Chem. Rev.*, vol. 117, no. 15, pp. 10212-10290, 2017, doi: 10.1021/acs.chemrev.7b00074.

[21] W. Zhu *et al.*, "Rapid continuous 3D printing of customizable peripheral nerve guidance conduits," *Mater. Today*, vol. 21, no. 9, pp. 951-959, 2018, doi: 10.1016/j.mattod.2018.04.001.

[22] J. Liu, L. Cui, and D. Losic, "Graphene and graphene oxide as new nanocarriers for drug delivery applications," *Acta Biomater.*, vol. 9, no. 12, pp. 9243-9257, 2013, doi: 10.1016/j.actbio.2013.08.016.

[23] M. Daniele, "Graphene in neurosurgery : the beginning of a new era," vol. 10, pp. 615–625, 2015.

[24] K. Liao, Y. Lin, C. Macosko, and C. Haynes, "Cytotoxicity of graphene oxide and graphene in human erythrocytes and skin fibroblasts," *ACS Appl ied Mater. Interfaces*, vol. 3, no. 7, pp. 2607-2615, 2011, doi: 10.1021/am200428v.

[25] P. Prabhakaran and K.-S. Lee, "Photo-polymerization," in *Functional Polymers, Polymers and Polymeric Composites: A Reference Series*, M. A. J. Mazumder, S. H., and A.-A. A, Eds. Springer Nature Switzerland AG, 2019, pp. 1-53.

[26] P. Hu *et al.*, "Conjugated Bifunctional Carbazole-Based Oxime Esters: Efficient and Versatile Photoinitiators for 3D Printing under One- and Two-Photon Excitation,"

ChemPhotoChem, vol. 4, no. 3, pp. 224-232, 2020, doi: 10.1002/cptc.201900246.
[27] H. Quan, T. Zhang, H. Xu, S. Luo, J. Nie, and X. Zhu, "Photo-curing 3D printing technique and its challenges," *Bioact. Mater.*, vol. 5, no. 1, pp. 110-115, 2020, doi: 10.1016/j.bioactmat.2019.12.003.
[28] B. Steyrer, P. Neubauer, R. Liska, and J. Stampfl, "Visible light photoinitiator for 3D-printing of tough methacrylate resins," *Materials (Basel).*, vol. 10, no. 12, pp. 1-11, 2017, doi: 10.3390/ma10121445.
[29] B. Zeng *et al.*, "Cytotoxic and cytocompatible comparison among seven photoinitiators-triggered polymers in different tissue cells," *Toxicol. Vitr.*, vol. 72, no. October 2020, 2021, doi: 10.1016/j.tiv.2021.105103.
[30] C.C. Wang, J.Y. Chen, and J. Wang, "The selection of photoinitiators for photopolymerization of biodegradable polymers and its application in digital light processing additive manufacturing," *J. Biomed. Mater. Res. – Part A*, vol. 110, no. 1, pp. 204-216, 2022, doi: 10.1002/jbm.a.37277.
[31] J. Guit *et al.*, "Photopolymer Resins with Biobased Methacrylates Based on Soybean Oil for Stereolithography," *ACS Appl. Polym. Mater.*, vol. 2, no. 2, pp. 949-957, 2020, doi: 10.1021/acsapm.9b01143.
[32] K.S. Lee and J.H. Lee, "Hybrid Thermal Recovery Using Low-Salinity and Smart Waterflood," *Hybrid Enhanc. Oil Recover. using Smart Waterflooding*, pp. 129-135, 2019, doi: 10.1016/b978-0-12-816776-2.00006-4.
[33] F. Wajdi, I. Kusumaningtyas, A.R. Wijaya, and A.E. Tontowi, "Graphene synthesis in obtaining a safe particle size in blood circulation system," *Res. J. Pharm. Technol.*, vol. 14, no. 1, pp. 270-274, 2021, doi: 10.5958/0974-360x.2021.00048.2.
[34] J.H. Sandoval, R.B. Wicker, J.H. Sandoval, and R.B. Wicker, "Functionalizing stereolithography resins : effects of dispersed multi-walled carbon nanotubes on physical properties," *Rapid Prototyp. J.*, vol. 12, no. 5, pp. 292-303, 2006, doi: 10.1108/13552540610707059.
[35] Y. Arao and M. Kubouchi, "High-rate production of few-layer graphene by high-power probe sonication," *Carbon N. Y.*, vol. 95, pp. 802-808, 2015, doi: 10.1016/j.carbon.2015.08.108.
[36] Z. Feng, Y. Li, C. Xin, D. Tang, W. Xiong, and H. Zhang, "Fabrication of Graphene-Reinforced Nanocomposites with Improved Fracture Toughness in Net Shape for Complex 3D Structures via Digital Light Processing," *J. Carbon Res.*, vol. 5, no. 25, pp. 1-16, 2019, doi: 10.3390/c5020025.
[37] R.G. Pauck and B.D. Reddy, "Computational analysis of the radial mechanical performance of PLLA coronary artery stents," *Med. Eng. Phys.*, vol. 37, no. 1, pp. 7-12, 2015, doi: 10.1016/j.medengphy.2014.09.014.
[38] G. Gonzalez *et al.*, "Development of 3D printable formulations containing CNT with enhanced electrical properties," *Polymer (Guildf).*, vol. 109, pp. 246-253, 2017, doi: 10.1016/j.polymer.2016.12.051.

Farid Wajdi
ORCID ID: 0000-0001-7624-7833
Department of Industrial Engineering
Universitas Serang Raya, Indonesia
e-mail: faridwajdi@unsera.ac.id

Alva Edy Tontowi (corresponding author)
ORCID ID: 0000-0002-1083-8961
Department of Mechanical and Industrial Engineering
Universitas Gadjah Mada, Indonesia
e-mail: alvaedytontowi@ugm.ac.id